# Effect of size and volume fraction of cuboidal γ' precipitates on mechanical properties of single crystal nickel-based superalloy CMSX-4

J. Lapin[1]*, M. Gebura[1], O. Bajana[1], T. Pelachová[1], M. Nazmy[2]

[1] *Institute of Materials and Machine Mechanics, Slovak Academy of Sciences, Račianska 75, 831 02 Bratislava, Slovak Republic*
[2] *ALSTOM Ltd., Department of Materials Technology, TTTM, CH-5401 Baden, Switzerland*

Received 20 March 2009, received in revised form 11 May 2009, accepted 13 May 2009

**Abstract**

The effect of size and volume fraction of cuboidal γ'($Ni_3$(Al,Ti)) precipitates on Vickers hardness and tensile properties at 950 °C of a single crystal nickel-based superalloy CMSX-4 was studied. Samples with a mean size and volume fraction of the cuboidal γ' precipitates ranging from 147 to 487 nm and from 62 to 70 vol.%, respectively, were prepared by heat treatment consisting of solution annealing, quenching and ageing at a temperature of 950 °C for various time ranging from 100 to 2000 h. Both the Vickers hardness $HV$ and 0.2 % offset yield strength $\sigma_{0.2}$ linearly decrease with decreasing normalized volume fraction $V_p$ and increasing normalized mean size $a$ of the γ' precipitates according to relationships $HV \propto \sqrt{V_p/a}$ and $\sigma_{0.2} \propto \sqrt{V_p/a}$, respectively. A linear relationship between the $\sigma_{0.2}$ and $HV$ is determined which allows high-temperature yield strength to be predicted from simple Vickers hardness measurements at room temperature. Critical resolved shear stress (CRSS) $\tau_{CRSS}$ is calculated to increase from 116 to 234 MPa by decreasing a mean width of the γ (Ni-based solid solution) channels from 71 to 32 nm. The decrease of 0.2 % yield strength with decreasing normalized volume fraction and increasing normalized size of the γ' precipitates is controlled by a decrease of order stress resulting from shearing of the γ' precipitates at high tensile stresses. The theoretical calculations validated by experimental results are used to predict ageing time and mean size of the γ' precipitates to achieve a peak 0.2 % tensile yield strength of the studied alloy at 950 °C.

K e y w o r d s: nickel alloys, single crystal superalloy, ageing, microstructure, mechanical properties

## 1. Introduction

Single crystal nickel-based superalloys are used in first-stage turbine blades because of their unusual ability to retain excellent combination of mechanical properties and corrosion resistance at high temperatures [1–8] comparing with other materials such as single or multiphase nickel-based intermetallics [9–12], titanium-based alloys [13–17] and iron-based intermetallics [18–21]. The typical microstructure of single crystal superalloys usually contains $L1_2$-ordered γ'($Ni_3$(Al,Ti)) precipitates coherently embedded in γ (Ni-based solid solution) matrix with face-centered cubic crystal structure. The mechanical properties of these materials depend on the volume fraction, distribution, size and morphology of the γ' precipitates. During service the initial microstructure of single crystal blades is subjected to degradation by the combined effect of temperature, mechanical stresses and environmental conditions. Three types of microstructure degradation can be observed in nickel-based superalloys exposed to high temperatures: (i) growth of γ' precipitates; (ii) spontaneous rafting formed preferentially within the dendrites during long-term ageing and (iii) creep rafting [4, 22–24]. The microstructure degradation resulting from the growth of γ' precipit-

*Corresponding author: tel.: +421 2 49268290; fax: +421 2 44253301; e-mail address: ummslapi@savba.sk

ates represents an important contribution to all degradation processes affecting performance and service life of critical gas turbine components such as first--stage turbine blades. Hence, it is important to study the effect of size and volume fraction of γ' precipitates on mechanical properties of single crystal superalloys at temperatures corresponding to those of turbine components.

The aim of the present work is to study the effect of size and volume fraction of cuboidal γ' precipitates on mechanical properties of single crystal nickel-based superalloy CMSX-4. The studied nickel-based superalloy is mainly used in manufacturing single crystal first--stage turbine blades for aircraft engines and stationary gas turbines for power engineering. The growth of the cuboidal γ' precipitates is observed in airfoil part of turbine blade subjected to high stresses and lower temperatures.

## 2. Experimental procedure

The superalloy CMSX-4 with the chemical composition Ni-7.0Cr-9.0Co-0.6Mo-6.0W-7.0Ta-3.0Re-5.6Al-1.0Ti-0.1Hf (wt.%) was provided by Cannon Muskegon (USA) in the form of a cylindrical ingot with a diameter of 60 mm and a length of 110 mm. The ingot was cut to smaller pieces using spark machining and lathe machined to cylindrical rods with a diameter of 11 mm and a length of 110 mm. Single crystal samples were prepared by seeding using seeds with [001] crystallographic orientation. Both the seed and cylindrical rod were put into a high--purity (99.95 %) alumina mould with a diameter of 11/15 mm (inside/outside diameter) and directionally solidified (DS) in a modified Bridgman type apparatus described elsewhere [25]. All samples were directionally solidified at a constant growth rate of $V = 2.78 \times 10^{-5}\,\mathrm{m\,s^{-1}}$ and constant temperature gradient in liquid at the solid-liquid interface of $G_\mathrm{L} = 8 \times 10^{3}\,\mathrm{K\,m^{-1}}$ under argon atmosphere (purity 99.995 %).

After directional solidification the single crystal samples were subjected to heat treatments consisting of solution annealing at 1315 ℃ for 6 h, fast gas cooling to room temperature and precipitation ageing at 950 ℃ for various time ranging from 100 to 2000 h.

Vickers hardness measurements were performed at an applied load of 298 N after each ageing step. Cylindrical tensile specimens with a gauge diameter of 5 mm and gauge length of 25 mm were prepared by lathe machining and grinding. The longitudinal axis of the tensile specimens was parallel or nearly parallel (maximum deviation of 3 degrees) to [001] crystallographic direction. Tensile tests were conducted at a temperature of 950 ℃ at an initial strain rate of $1 \times 10^{-4}\ \mathrm{s^{-1}}$ using universal testing machine Zwick in air. The elongation was measured by high-temperature extensometer Maytec (resolution of 0.1 μm) touching gauge section of the tensile specimens. The offset tensile yield strength was measured at 0.2 % plastic strain and ductility was evaluated from the total plastic elongation to fracture.

Crystallographic orientation of each single crystal was determined by a Laue diffraction method. Microstructural analysis was performed by light optical microscopy (OM), scanning electron microscopy (SEM) and transmission electron microscopy (TEM). OM and SEM samples were prepared using standard metallographic techniques and etched in a reagent of 12.5 ml alcohol, 12.5 ml $HNO_3$ and 13.5 ml HCl. TEM samples (thin carbon replicas) were prepared by deposition of thin carbon layer on an etched surface, which was then removed from the surface by electrolytic etching in a solution of 9.4 ml $H_3PO_4$, 37.5 ml $H_2SO_4$ and 35.6 ml $HNO_3$ at a voltage of 7 V. Size and volume fraction of γ' precipitates and γ channels was measured on digitalized micrographs using a computerized image analyser.

## 3. Results

### 3.1. Effect of ageing time on size and volume fraction of γ' precipitates

Figure 1 shows the typical morphology of the γ' precipitates after solution annealing at 1315 ℃ for 6 h and precipitation ageing at 950 ℃ for various time ranging from 100 to 2000 h. Nearly square section on {001} crystallographic planes indicates that the cuboidal morphology of the γ' precipitates is retained up to ageing time of 2000 h, as shown in Figs. 1a and 1b. Morphological stability of the cuboidal γ' precipitates can be evaluated from their shape factor $F$ defined as

$$F = \frac{4\pi A}{P^2}, \tag{1}$$

where $A$ and $P$ is the cross sectional area and perimeter of the γ' precipitate on {001} crystallographic planes, respectively. The shape factor is calculated to vary between 0.772 and 0.791, which are very close values to that of 0.785 calculated for an ideal square and confirm morphological stability of the γ' precipitates during ageing. The measured statistical data (minimum 1000 precipitates measured at each ageing time) of size of the cuboidal γ' precipitates defined as their edge length $a_\mathrm{m}$ can be fitted by a log-normal distribution function $\varphi(a_\mathrm{m})$ in the form

$$\varphi\left(a_\mathrm{m}\right) = \frac{1}{\sigma_\mathrm{s}\sqrt{2\pi}} \exp\left[-\frac{\left(\ln a_\mathrm{m} - \ln a\right)^2}{2\sigma_\mathrm{s}^2}\right], \tag{2}$$

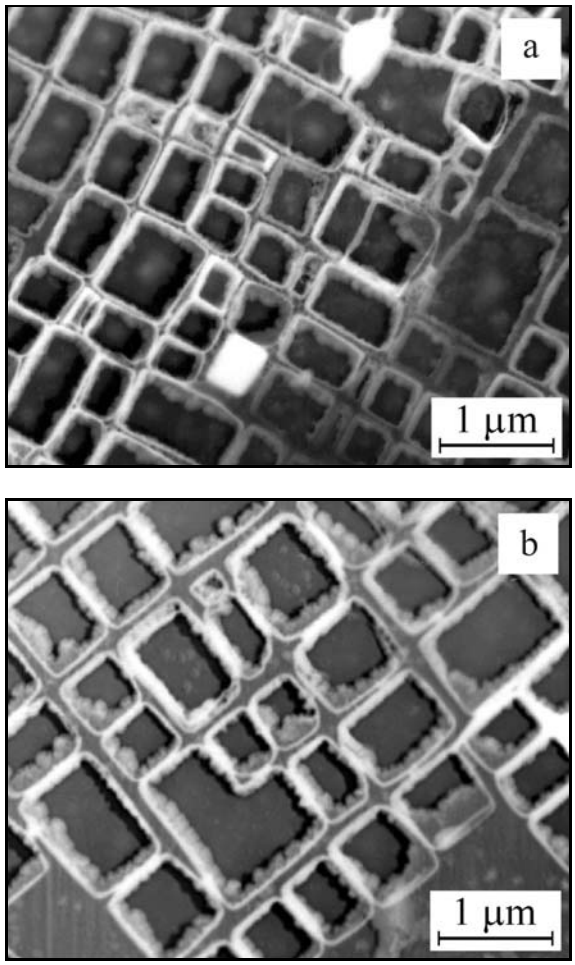


Fig. 1. TEM micrographs showing the effect of ageing at 950 °C on morphology and size of the γ' precipitates on {001} crystallographic planes: (a) 1030 h, (b) 2000 h.

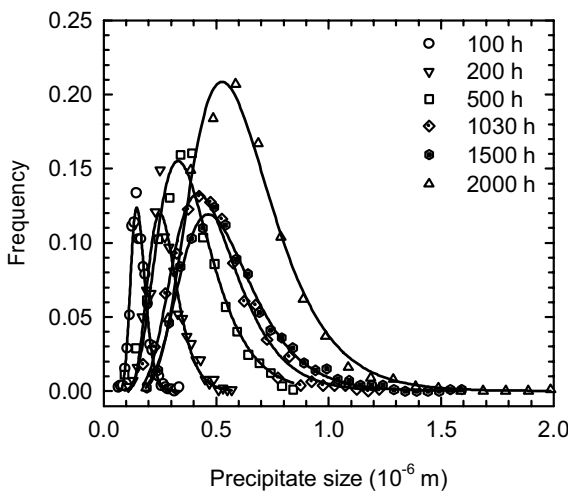


Fig. 2. Log-normal distribution curves for size of cuboidal γ' precipitates after ageing at 950 °C. The ageing times are indicated in the figure.

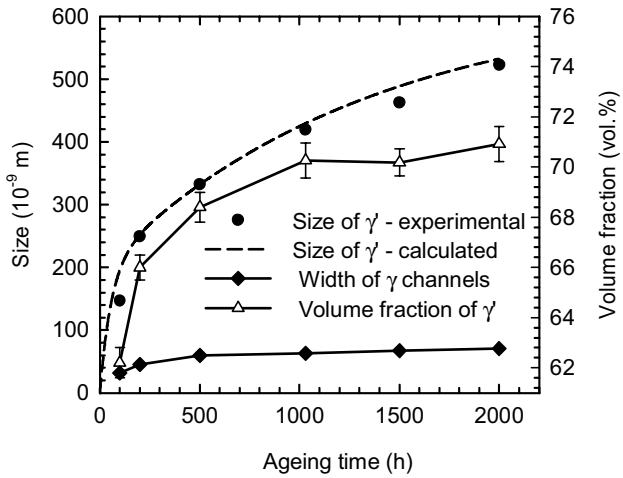


Fig. 3. Dependence of mean size and volume fraction of cuboidal γ' precipitates and mean width of γ channels on ageing time. Calculated values of the mean size of γ' precipitates according to Eq. (4) are indicated in the figure by a dashed line.

where $a$ is the mean size and $\sigma_s$ is the variance of log-normal distribution. Figure 2 shows log-normal distribution curves resulting from the statistical evaluation of the size of γ' precipitates after ageing at 950 °C. Figure 3 shows dependence of mean size and volume fraction of the γ' precipitates and mean width of γ channels on the ageing time. The mean size $a$ of the γ' precipitates, width of γ channels $w_\gamma$ and volume fraction $V_p$ of the γ' precipitates increase with increasing ageing time.

### 3.2. Effect of ageing time on mechanical properties

Figure 4 shows dependence of Vickers hardness on ageing time. Continuous decrease of the Vickers hardness with increasing ageing time indicates that even a mean size of the γ' precipitates of $a = 147$ nm after ageing for 100 h is larger than that required to achieve peak hardness values, e. g. all studied samples subjected to evaluation of mechanical properties were over-aged.

Figure 5 shows examples of the typical tensile stress-strain curves at 950 °C. All specimens show smooth increase of the stress with strain to a maximum stress at a strain of about 2 % and then smooth decrease of the stress with the increasing strain up to fracture. No clear yielding was observed during tensile testing. Figure 6 shows evolution of 0.2 % offset yield strength ($\sigma_{0.2}$), ultimate tensile strength (UTS) and plastic elongation to fracture with ageing time. The yield strength decreases with increasing ageing time, which is similar behaviour to that of the Vickers hardness with the ageing time (see Fig. 4). On the other

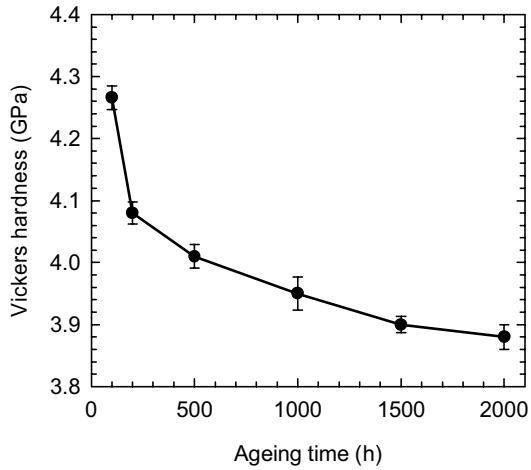


Fig. 4. Dependence of Vickers hardness on ageing time.

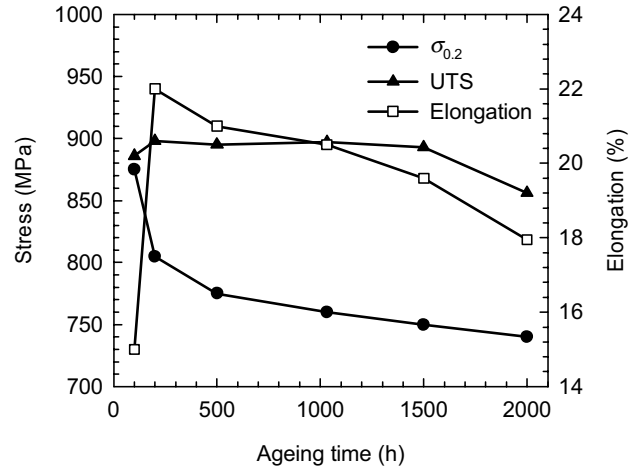


Fig. 6. Effect of ageing time on 0.2 % offset yield strength ($\sigma_{0.2}$), UTS and plastic elongation to fracture at 950 ℃.

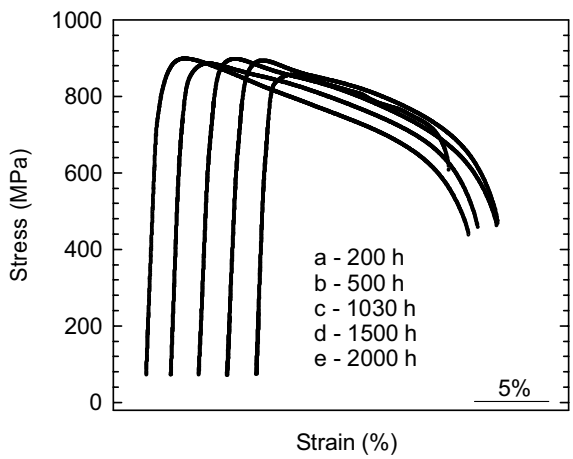


Fig. 5. Examples of the typical tensile stress-strain curves for specimens with cuboidal γ' precipitates at 950 ℃. The ageing times are indicated in the figure.

hand, both UTS and plastic elongation to fracture first increase and then decrease with increasing ageing time. It should be noted that the data shown in Fig. 6 represent average values from two tensile specimens tested at each ageing regime.

## 4. Discussion

### 4.1. Coarsening of cuboidal γ' precipitates during ageing at 950℃

As shown recently by Lapin et al. [4], the mean size $a$ of the cuboidal γ' precipitates in single crystal superalloy CMSX-4 subjected to isothermal ageing at temperatures ranging from 850 to 1000 ℃ can be calculated according to a standard Lifshitz-Slyozov-Wagner kinetic equation in the form [26]

$$a^3 - a_0^3 = \frac{64 C_\infty \sigma_{\gamma/\gamma'} \Omega^2 D_{\text{eff}} t}{9RT}, \qquad (3)$$

where $a_0$ is the initial size of the cuboidal γ' precipitates at ageing time $t = 0$ s, $C_\infty$ is the molar solid solubility of controlling solute in the matrix, $\sigma_{\gamma/\gamma'}$ is the γ/γ' interfacial energy, $\Omega$ is the molar volume of the γ' precipitate, $t$ is the ageing time, $R$ is the universal gas constant, $T$ is the absolute temperature and $D_{\text{eff}}$ is the effective diffusion coefficient. It was shown that the values of $a$ calculated according to Eq. (3) at 950 ℃ are in a very good agreement with experimentally measured ones for the samples with an initial size of the cuboidal γ' precipitates of about $a_0 = 300$ nm and taking the effective diffusion coefficient of $D_{\text{eff}} = 9.41 \times 10^{-17}\,\text{m}^2\,\text{s}^{-1}$, molar solubility of Al in the γ matrix of $C_\infty = 10447\,\text{mol}\,\text{m}^{-3}$ and γ/γ' interfacial energy of $\sigma_{\gamma/\gamma'} = 41.365\,\text{mJ}\,\text{m}^{-2}$ [4, 27]. However, the validity of Eq. (3) and above mentioned physical data was not verified for the samples subjected to different heat treatments and early stages of coarsening process.

We will assume that after fast gas cooling of the samples from solution annealing temperature of 1315 ℃ the initial size of the γ' precipitates $a_0$ is very small and can be neglected in Eq. (3). Hence, the size of the γ' precipitates $a$ at ageing time $t$ can be calculated as follows

$$a = \sqrt[3]{\frac{64 C_\infty \sigma_{\gamma/\gamma'} \Omega^2 D_{\text{eff}} t}{9RT}}. \qquad (4)$$

Figure 3 shows the calculated size of cuboidal γ' precipitates $a$ (in m) according to Eq. (4) and taking

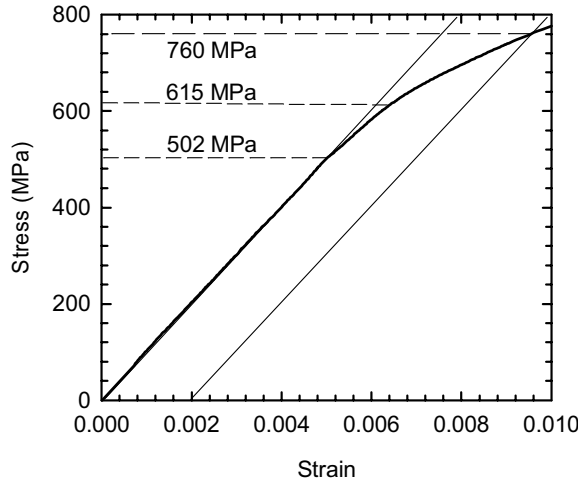


Fig. 7. Detail of stress-strain diagram showing elastic region and microplasticity region in the vicinity of the offset yield strength.

$C_\infty = 10447\,\mathrm{mol\,m^{-3}}$, $\sigma_{\gamma/\gamma'} = 4.1365 \times 10^{-2}\,\mathrm{J\,m^{-2}}$, $\Omega = 2.734 \times 10^{-5}\,\mathrm{m^3\,mol^{-1}}$, $D_{\mathrm{eff}} = 9.41 \times 10^{-17}\,\mathrm{m^2\,s^{-1}}$, $R = 8.314\,\mathrm{J\,K^{-1}\,mol^{-1}}$, $T = 1223\,\mathrm{K}$ and applied ageing time $t$ ranging from $3.6 \times 10^5$ to $7.2 \times 10^6$ s. It is clear that experimentally measured mean values of size of the $\gamma$' precipitates $a$ cluster around the calculated ones indicated by a dash line. Such excellent agreement between measured and calculated values extends the validity of coarsening kinetic equation for cuboidal $\gamma$' precipitates in CMSX-4 superalloy defined by Lapin et al. [4] and confirms validity of the effective diffusion coefficients $D_{\mathrm{eff}}$ and $\gamma/\gamma$' interfacial energy $\sigma_{\gamma/\gamma'}$ estimated recently by the authors.

### 4.2. Effect of size and volume fraction of cuboidal $\gamma$' precipitates on high-temperature yield strength and room-temperature hardness

Figure 7 shows a detail of the tensile stress-strain curve of the specimen with a mean size of cuboidal $\gamma$' precipitates of $a = 420\,\mathrm{nm}$, which will be used as the typical example to estimate contribution of each strengthening mechanism to 0.2 % offset yield strength. The tensile curve shows an apparently elastic region up to a stress of about 502 MPa, which is followed by the first region of plastic deformation up to a stress of about 615 MPa and the second region of the plastic deformation up to the 0.2 % offset yield strength of 760 MPa.

It has been convincingly demonstrated that the tensile deformation of single crystal superalloys at high temperatures is essentially confined in the $\gamma$ channels on {111} slip planes and <110> slip directions [27–30]. Before the dislocation can be moved through the $\gamma$ phase, the applied stress must be high enough to overcome the local Orowan resistance, solid solution resistance and dislocation resistance of the $\gamma$ matrix [28–30].

#### *4.2.1. Orowan resistance to dislocation motion*

Pollock et al. [28] and Ma et al. [29] estimated Orowan stress $\tau_{\mathrm{or}}$ from a simplified relationship in the form

$$\tau_{\mathrm{or}} = \frac{G_\gamma b_\gamma}{\lambda}, \tag{5}$$

where $G_\gamma$ is the shear modulus of the $\gamma$ matrix, $b_\gamma$ is the length of Burgers vector and $\lambda$ is the width of $\gamma$ channel in the slip plane. More complex analysis of Orowan stress based on line tension of edge and screw dislocations was performed by Benyoucef et al. [30]. Lapin and Delannay [31] calculated Orowan stress taking into account line tension of edge and screw dislocations and assumption that the overall passing stress is the geometrical mean of the critical bowing stresses for edge and screw dislocations according to relationship

$$\tau_{\mathrm{or}} = \frac{G_\gamma b_\gamma}{2\pi\lambda\sqrt{1-\nu}} \ln\frac{\lambda}{2r}, \tag{6}$$

where $\nu$ is the Poisson's ratio and $r$ is the inner cut-off radius of dislocation. Assuming Eq. (6) and taking $G_\gamma = 36.1\,\mathrm{GPa}$ [26], $\nu = 0.422$ [32], $\lambda$ values calculated from the width of the $\gamma$ channels $w_\gamma$ shown in Fig. 3 and inner cut of radius of dislocation of $r = 2.54 \times 10^{-10}$ m [31], one can calculate that the Orowan stress decreases from 214 to 96 MPa by increasing mean size of width of the $\gamma$ channels from 32 to 71 nm. For the tensile specimen with the mean size of the precipitates of $a = 420\,\mathrm{nm}$, one can calculate $\tau_{\mathrm{or}} = 108\,\mathrm{MPa}$. Figure 8 shows dependence of Orowan stress $\tau_{\mathrm{or}}$ calculated according to Eq. (6) on normalized volume fraction and size of the cuboidal $\gamma$' precipitates. The reason of selecting $x$-axis in the form $(V_{\mathrm{p}}/a)^{0.5}$ and not in the form of the width of the $\gamma$ channels will be explained later in this chapter. The Orowan stress increases with increasing normalized volume fraction and decreasing normalized size of the precipitates.

#### *4.2.2. Solid solution and dislocation resistance*

The additional factor that increases resistance to dislocation motion in the $\gamma$ channels is the friction stress $\tau_{\mathrm{ss}}$ resulting from solid solution strengthening of the $\gamma$ phase. We can refer to a value of about 20 MPa, which was derived by Pollock and Argon [28] and also used by Ma et al. [29].

The stress resulting from the dislocation resistance $\tau_d = 10$–$12$ MPa was estimated by Pollock and Argon [28] during steady-state creep at 850 °C of CMSX-3 superalloy. However, Lukáš et al. [33] showed that the dislocation density in heat-treated CMSX-4 superalloy was very small before testing. Hence, the stress resulting from the dislocation resistance $\tau_d$ must be significantly lower than that of 10–12 MPa resulting from the analysis of Pollock and Argon [28] and its contribution to CRSS can be neglected.

#### 4.2.3. Misfit stress

The additional parameter affecting movement of dislocations through the $\gamma$ channels is misfit stress $\sigma_m$. The misfit stress results from the lattice misfit $\delta$ defined as

$$\delta = \frac{2\left(a_{\gamma'} - a_\gamma\right)}{a_{\gamma'} + a_\gamma}, \tag{7}$$

where $a_{\gamma'}$ and $a_\gamma$ are the lattice parameters of the $\gamma$' and $\gamma$ phases, respectively. Ma et al. [29] proposed for calculation of average misfit stress in the $\gamma$' precipitates relationship in the form

$$\langle\sigma_m\rangle_{\gamma'} = -\left(1 - V_p\right)\frac{2E_{\gamma'}}{3\left(1-\nu_{\gamma'}\right)}\Delta\alpha\Delta T, \tag{8}$$

where $E_{\gamma'}$ is the Young's modulus of the $\gamma$' phase in [001] crystallographic direction, $\nu_{\gamma'}$ is the Poisson's ratio of the $\gamma$' phase, $\Delta\alpha = \alpha_{\gamma'} - \alpha_\gamma$ is the difference between the coefficient of the thermal expansion of the $\gamma$' ($\alpha_{\gamma'}$) and $\gamma$ ($\alpha_\gamma$) phases and $\Delta T = T - T_0$ is the difference between the test temperature $T$ and the reference temperature $T_0$. For the $\gamma$ phase, an average misfit stress can be calculated as follows:

$$\langle\sigma_m\rangle_\gamma = V_p\frac{2E_\gamma}{3\left(1-\nu_\gamma\right)}\Delta\alpha\Delta T, \tag{9}$$

where $E_\gamma$ is the Young's modulus of the $\gamma$ phase in [001] crystal direction and $\nu_\gamma$ is the Poisson's ratio of the $\gamma$ phase. Unconstrained thermal misfit $\Delta\alpha\Delta T$ can be related to the constrained lattice misfit $\delta$ as follows [29]:

$$\delta = \frac{1+\nu}{3\left(1-\nu\right)}\Delta\alpha\Delta T. \tag{10}$$

Using the method of Ma et al. [29] and taking a constrained misfit for CMSX-4 superalloy of $\delta = -0.0028$ between RT and 950 °C [34], Poisson's ratio $\nu_\gamma = 0.422$ [32], Young's modulus of $E_\gamma = 80$ GPa [32], one can calculate an average compression stress parallel to the planes of interface in the $\gamma$ channels of $\sigma_m = -220$ MPa. For the $\gamma$' precipitates, an average tensile stress of $\sigma_m = 100$ MPa parallel to the interface can be calculated by taking $\nu_{\gamma'} = 0.434$ and $E_{\gamma'} = 85$ GPa [30]. It should be noted that Ma et al. [29] calculated an average misfit compressive stress of $-93$ MPa and tensile stress of 50 MPa for the $\gamma$ channels and $\gamma$' precipitates, respectively, in PWA 1422 superalloy at 900 °C. For CMSX-3 superalloy, Pollock and Argon [28] calculated compressive stress of $-433$ MPa and tensile stress of 50 MPa for the $\gamma$ channels and $\gamma$' precipitates, respectively. While the misfit stresses are highly non-uniform in the $\gamma$ channels, they are quite uniform in the bulk $\gamma$' precipitates [29]. In the case of a superalloy with a negative misfit (e.g. CMSX-4), the misfit induced compression stress $\sigma_m$ in the horizontal $\gamma$ channels (the channels perpendicular to load direction) complements the applied tensile stress $\sigma_a$ and increases resolved shear stress (RSS) $\tau^H_{RSS}$ according to relationship in the form [29]:

$$\tau^H_{RSS} = (\sigma_a + \sigma_m)\cos 45\cos 54.74. \tag{11}$$

On the other hand, RSS $\tau^V_{RSS}$ in the vertical $\gamma$ channels (parallel to load direction) depends completely on the applied load according to relationship in the form [29]:

$$\tau^V_{RSS} = \{(\sigma_a - \sigma_m) + \sigma_m\}\cos 45\cos 54.74. \tag{12}$$

#### 4.2.4. Critical resolved shear stress

Critical resolved shear stress (CRSS) $\tau_{CRSS}$ can be expressed in the form

$$\tau_{CRSS} = \tau_{or} + \tau_{ss} + \tau_d. \tag{13}$$

From the above-mentioned estimates, one can calculate increase of $\tau_{CRSS}$ from 116 to 234 MPa by decreasing width of the $\gamma$ channels from 71 to 32 nm.

Assuming the specimens with a mean size of the $\gamma$' precipitates of $a = 420$ nm, the CRSS is $\tau_{CRSS} = 128$ MPa, which corresponds to an applied tensile stress of 314 MPa. According to Eq. (11) and taking calculated CRSS of $\tau_{CRSS} = 128$ MPa and for the simplicity only average misfit stress of 220 MPa, an applied stress of $\sigma_a = 94$ MPa is required to move the dislocations through the horizontal $\gamma$ channels. However, to achieve measurable plastic strain in the tension test, the dislocations must glide on both channels. Hence the applied stress must achieve a value of $\sigma_a = 314$ MPa, which is significantly lower than the observable limit of elasticity of about 502 MPa observed on the stress-strain curve shown in Fig. 7. Similar discrepancy between the CRSS and saturation of an elastic limit on stress-strain curve was observed also by Ma et al. [29] in PWA 1422 superalloy at 900 °C. However, using neutron diffraction, these

authors demonstrated that the elastic strain in the γ phase saturates at a stress of about 350 MPa, which is well below the observable elastic limit (of about 500 MPa) resulting from the tensile stress-strain curve and this elastic limit corresponds very well to the CRSS.

The CRSS, which is dominated by the Orowan stress, is extremely important parameter in analysis of creep behaviour of the superalloys. The fact that the γ' precipitates remain largely elastic during creep reduce significantly the RSS in the vertical channels. The dislocation gliding is limited to the horizontal channels because of the negative misfit at low and moderate applied stresses. Such anisotropic character of dislocation distribution formed during primary and secondary creep affects creep behaviour as well as microstructural stability of the superalloys.

### 4.2.5. Order strengthening

Strengthening by the ordered coherent γ' precipitates occurs when a matrix dislocation shears an ordered precipitate and creates an antiphase boundary on the slip plane of the precipitate. The antiphase boundary energy $\gamma_{\mathrm{APB}}$ represents the force opposing the motion of the dislocation as it penetrates the particle. Figure 7 indicates that the slope of the stress-strain curve changes at about 615 MPa, which might be associated with the load transfer from the γ phase to the γ' phase. The CRSS that is required to insert a pair of γ dislocations into the γ' precipitates $\tau_{\mathrm{CRSS}\gamma'}$ is defined as

$$\tau_{\mathrm{CRSS}\gamma'} = \frac{\gamma_{\mathrm{APB}}}{2b}. \tag{14}$$

The antiphase boundary energy for the γ' phase in the CMSX-4 superalloy was measured to be $\gamma_{\mathrm{APB}} = (150 \pm 15)\,\mathrm{mJ\ m^{-2}}$ [35]. We thus arrive to $\tau_{\mathrm{CRSS}\gamma'} = 295 \pm 30$ MPa. Assuming crystallographic orientation of the tensile specimen, the corresponding tensile stress required to shear cuboidal γ' precipitates is 614 ± 63 MPa, which corresponds very well to the value of 615 MPa shown in Fig. 7. After achieving a stress necessary to shear the γ' precipitates, the CMSX-4 behaves as the typical overaged alloy. The contribution of the order strengthening to RSS $\tau_{\mathrm{s}}$ for an overaged alloy can be calculated according to equation in the form [36]

$$\tau_{\mathrm{s}} = 0.7\sqrt{\frac{wT_{\mathrm{L}}V_{\mathrm{p}}\gamma_{\mathrm{APB}}}{b^2 a}}, \tag{15}$$

where $w$ is the parameter, which accounts for the repulsion of the dislocation within the precipitates, and $T_{\mathrm{L}}$ is the line tension of dislocation. The parameter

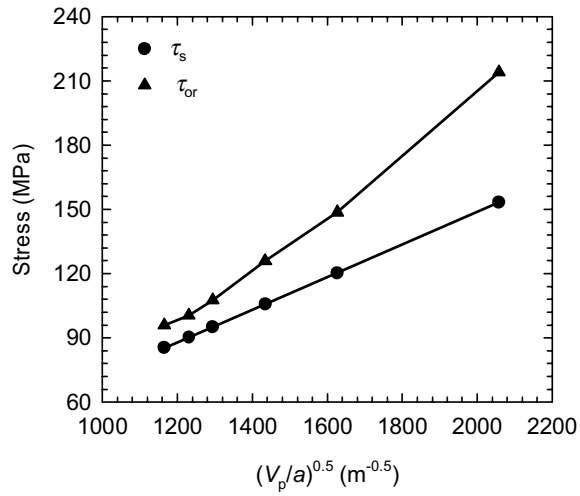


Fig. 8. Dependence of Orowan shear stress $\tau_{\mathrm{or}}$ and RSS stress resulting from shearing of the γ' precipitates $\tau_{\mathrm{s}}$ on normalized volume fraction $V_{\mathrm{p}}$ and size $a$ of the cuboidal γ' precipitates.

$w$ is essentially an adjustable parameter, which is required to produce agreement between theory and experiment. The line tension of dislocation is defined as [36]:

$$T_{\mathrm{L}} = \frac{G_\gamma b_\gamma^2}{4\pi}\left(\frac{1+\nu-3\nu\sin^2\xi}{1-\nu}\right)\ln\left(\frac{\lambda}{r}\right), \tag{16}$$

where $\xi$ is the angle between the dislocation line and its Burgers vector. Figure 8 shows dependence of RSS $\tau_{\mathrm{s}}$ calculated according to Eq. (15) and taking $w = 3$ on normalized volume fraction and size of cuboidal γ' precipitates. Linear regression analysis of data shown in Fig. 8 yields an equation for $\tau_{\mathrm{s}}$ in the form

$$\tau_{\mathrm{s}} = -3.41 + 7.61 \times 10^{-2}\sqrt{\frac{V_{\mathrm{p}}}{a}}. \tag{17}$$

Correlation coefficient of this fit is $r^2 = 0.99$.

Assuming weak dependence of line tension of dislocation on microstructural parameters, Eq. (15) can be rewritten in a simplified form

$$\tau_{\mathrm{s}} \approx A\sqrt{\frac{V_{\mathrm{p}}}{a}}, \tag{18}$$

where $A$ is a constant. Figure 9 shows dependence of experimentally measured RSS $\tau_{0.2}$ corresponding to the offset 0.2 % yield strength, yield strength $\sigma_{0.2}$ and Vickers hardness on normalized size and volume fraction of the cuboidal γ' precipitates. The RSS $\tau_{0.2}$ increases proportionally with decreasing size and increasing volume fraction of the γ' precipitates. Linear

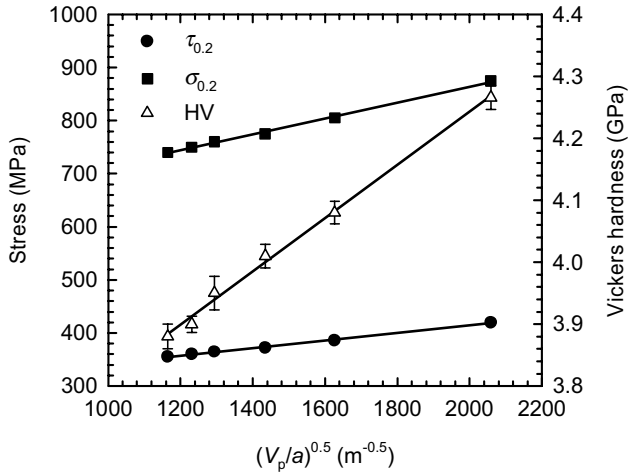


Fig. 9. Dependence of RSS $\tau_{0.2}$, 0.2 % offset yield strength $\sigma_{0.2}$ and Vickers hardness $HV$ on normalized volume fraction $V_\mathrm{p}$ and size $a$ of the cuboidal $\gamma$' precipitates.

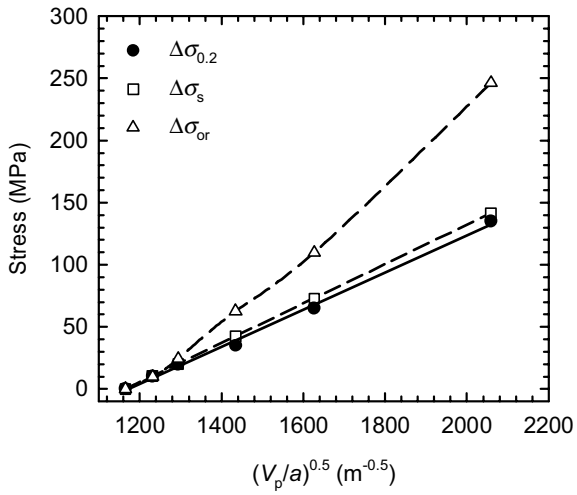


Fig. 10. Dependence of a decrease of 0.2 % offset yield strength $\Delta\sigma_{0.2}$, decrease of order stress resulting from shearing of $\gamma$' precipitates $\Delta\sigma_\mathrm{s}$ and decrease of Orowan stress $\Delta\sigma_\mathrm{or}$ on normalized volume fraction $V_\mathrm{p}$ and size $a$ of the cuboidal $\gamma$' precipitates.

regression analysis of data shown in Fig. 9 yields an equation for $\tau_{0.2}$ in the form

$$\tau_{0.2} = 271 + 7.2 \times 10^{-2}\sqrt{\frac{V_\mathrm{p}}{a}}, \tag{19}$$

for the 0.2 % offset tensile yield strength $\sigma_{0.2}$ in the form

$$\sigma_{0.2} = 564 + 0.15\sqrt{\frac{V_\mathrm{p}}{a}}, \tag{20}$$

and for Vickers hardness $HV$ we can write

$$HV = 3.38 + 4.3\sqrt{\frac{V_\mathrm{p}}{a}}. \tag{21}$$

The correlation coefficients of these fits are better than $r^2 = 0.98$.

Figure 10 shows dependence of a decrease of 0.2 % offset yield strength defined as $\Delta\sigma_{0.2} = \sigma_{0.2\mathrm{max}} - \sigma_{0.2}$, decrease of the stress resulting from order strengthening by the $\gamma$' precipitates defined as $\Delta\sigma_\mathrm{s} = \sigma_{\mathrm{s\,max}} - \sigma_\mathrm{s}$, and decrease of Orowan stress defined as $\Delta\sigma_\mathrm{or} = \sigma_{\mathrm{or\,max}} - \sigma_\mathrm{or}$ on normalized volume fraction and size of the cuboidal $\gamma$' precipitates. It is clear that the decrease of the offset yield strength $\Delta\sigma_{0.2}$ can be very well related to the decrease of the stress resulting from order strengthening $\Delta\sigma_\mathrm{s}$. On the other hand, decrease of the Orowan stress $\Delta\sigma_\mathrm{or}$ with the normalized volume fraction and size of the $\gamma$' precipitates deviates significantly from that of $\Delta\sigma_{0.2}$. Hence, the high-temperature 0.2 % offset yield strength of the studied alloy is largely controlled by stress contribution resulting from the order strengthening and not from Orowan bowing mechanism.

#### *4.2.6. Estimation of peak yield strength*

It is demonstrated that the studied CMSX-4 superalloy behaves as the typical overaged material strengthened by ordered precipitates characterized by a continuous decrease of the yield strength $\sigma_{0.2}$ with increasing size and decreasing volume fraction of the $\gamma$' precipitates. It is of interest to estimate optimal parameters required to achieve peak values of the yield strength. As suggested by Ardell [37], the stress contribution from shearing of peak aged precipitates $\tau_\mathrm{sp}$ to RSS can be calculated as

$$\tau_\mathrm{sp} = 0.81\frac{\gamma_\mathrm{APB}}{2b}\sqrt{\frac{3\pi V_\mathrm{p}}{8}}. \tag{22}$$

Taking volume fraction of the $\gamma$' precipitates $V_\mathrm{p}$ ranging from 0.62 to 0.70, one can calculate a peak stress $\tau_\mathrm{sp}$ resulting from the order strengthening to vary between 204 and 217 MPa. Taking these values and assuming validity of extrapolated values from Eq. (17), one can calculate a mean size of cuboidal $\gamma$' precipitates of $a = 84$ nm for a peak aged superalloy CMSX-4. In order to achieve such mean size of the $\gamma$' precipitates, the alloy should be aged for $t = 7.6$ h at 950 °C according to Eq. (4). Such theoretical estimates were experimentally verified by additional ageing experiments at 950 °C for different time ranging from 2 to 36 h. Figure 11 shows dependence of Vickers hardness on ageing time. It is clear that the peak hardness values are achieved after ageing for about

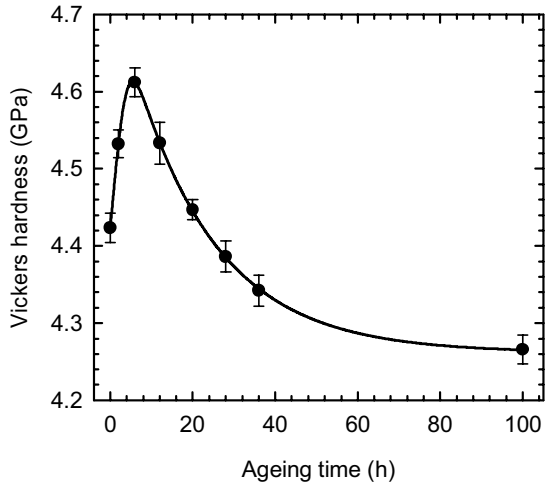


Fig. 11. Variation of Vickers hardness with the ageing time showing a fitting curve for a peak aged conditions.

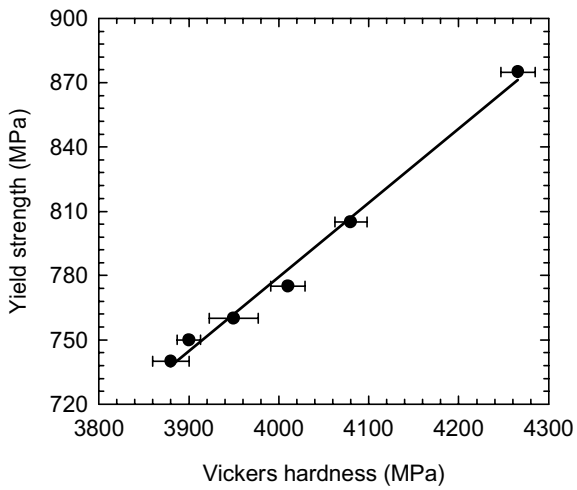


Fig. 12. Dependence of 0.2 % offset yield strength at 950 °C on room-temperature Vickers hardness.

6 h, which is a comparable value with that of 7.6 h resulting from the calculations. In addition, the mean size of the cuboidal γ' precipitates was measured to be $a = 82$ nm in the sample aged at 950 °C for 6 h, which is also in a good agreement with a predicted value of 84 nm calculated according to Eq. (4).

Both the yield strength $\sigma_{0.2}$ and Vickers hardness show linear dependence on normalized volume fraction and size of the γ' precipitates, as seen in Fig. 9. Figure 12 shows dependence of the offset yield strength $\sigma_{0.2}$ measured at 950 °C on room-temperature Vickers hardness $HV$. The yield strength $\sigma_{0.2}$ increases linearly with Vickers hardness $HV$ according to equation

$$\sigma_{0.2} = HV_0 + k_{\mathrm{HV}} HV, \tag{23}$$

where $HV_0$ is a constant (in MPa), $k_{\mathrm{HV}}$ is a dimensionless material constant and $HV$ is the Vickers hardness (in MPa). Linear regression analysis of data shown in Fig. 12 yields an equation for $\sigma_{0.2}$ in the form

$$\sigma_{0.2} = -607.4 + 0.347HV. \tag{24}$$

The correlation coefficient of this fit is $r^2 = 0.97$. According to Eq. (24) and taking $HV = 4610$ MPa measured for the peak aged samples, one can calculate 0.2 % peak yield strength of $\sigma_{0.2} = 991$ MPa. Hence, Eq. (24) can be considered as a simple tool to estimate high temperature yield strength from room-temperature measurements of Vickers hardness.

## 5. Conclusions

The investigation of the effect of size and volume fraction of cuboidal γ' precipitates on mechanical properties of single crystal nickel-based superalloy CMSX-4 suggests the following conclusions:

1. Heat treatments of single crystal samples consisting of solution annealing, quenching and ageing at 950 °C for various time from 100 to 2000 h lead to formation of cuboidal γ' ($Ni_3(Al,Ti)$) precipitates with a mean size and volume fraction ranging from 147 to 487 nm and from 62 to 70 vol.%, respectively. The mean size of the γ' precipitates can be very well predicted from a modified coarsening kinetic equation.

2. Both room-temperature Vickers hardness $HV$ and 0.2 % tensile yield strength $\sigma_{0.2}$ at 950 °C decrease with decreasing volume fraction $V_{\mathrm{p}}$ and increasing mean size $a$ of the γ' precipitates according to relationships $HV \propto (V_{\mathrm{p}}/a)^{0.5}$ and $\sigma_{0.2} \propto (V_{\mathrm{p}}/a)^{0.5}$, respectively. A linear relationship between the $\sigma_{0.2}$ and $HV$ was determined, which allows high-temperature yield strength to be predicted from simple Vickers hardness measurements at room temperature.

3. The critical resolved shear stress (CRSS) $\tau_{\mathrm{CRSS}}$ of the γ matrix is calculated to increase from 116 to 234 MPa by decreasing mean size of the γ channels from 71 to 32 nm. The CRSS is largely dominated by Orowan bowing of dislocation through the γ channels. While the CRSS is an important parameter in a creep regime of the studied alloy, decrease of 0.2 % tensile yield strength with decreasing volume fraction and increasing size of the γ' precipitates is controlled by a decrease of the order stress resulting from shearing of the γ' precipitates at high tensile stresses.

4. Mean size of the γ' precipitates and ageing time to achieve peak values of the yield strength are theoretically predicted and verified by additional ageing experiments at 950 °C and Vickers hardness measurements. It is found that a peak hardness values are achieved after ageing for about 6 h at 950 °C, which corresponds to a mean size of the γ' precipitates of

82 nm. These experimental values are in a good agreement with those predicted by calculations. The peak tensile yield strength $\sigma_{0.2}$ is estimated to achieve of about 991 MPa after a peak ageing of the studied alloy.

## Acknowledgements

This work was financially supported by the Slovak Grant Agency for Science under the contract VEGA 2/7085/27. The authors would like to express their gratitude to Dr. K. Harris from Cannon Muskegon Corporation (USA) for providing the ingot of CMSX-4 superalloy.

## References

[1] SERIN, K.—GÖBENLI, G.—EGGELER, G.: Mater. Sci. Eng. A, *387–389*, 2004, p. 133.
[2] MA, A.—DYE, D.—REED, R. C.: Acta Mater., *56*, 2008, p. 1657.
[3] MATAN, N.—COX, D. C. C.—RAE, M. F.—REED, R. C.: Acta Mater., *47*, 1999, p. 2031.
[4] LAPIN, J.—GEBURA, M.—PELACHOVÁ, T.—NAZMY, M.: Kovove Mater., *46*, 2008, p. 313.
[5] WAGNER, A.—SHOLLOCK, B. A.—MCLEAN, M.: Mater. Sci. Eng. A, *374*, 2004, p. 270.
[6] LUKÁŠ, P.—KUNZ, L.—SVOBODA, M.: Mater. Sci. Eng. A, *387–389*, 2004, p. 505.
[7] LUKÁŠ, P.—ČADEK, J.—ŠUSTEK, V.—KUNZ, L.: Mater. Sci. Eng. A, *208*, 1996, p. 149.
[8] KAMARAJ, M.—SERIN, K.—KOLBE, M.—EGGELER, G.: Mater. Sci. Eng. A, *319–321*, 2001, p. 796.
[9] KURSA, M.—MALCHARCZIKOVÁ, J.—PEŠIČKA, J.—VODÁREK, V.—HYSPECKÁ, L.: Kovove Mater., *46*, 2008, p. 351.
[10] LAPIN, J.—MAREČEK, J.: Intermetallics, *14*, 2006, p. 1339.
[11] LAPIN, J.: Scripta Mater., *51*, 2004, p. 733.
[12] LAPIN, J.—PELACHOVÁ, T.—BAJANA, O.: Intermetallics, *8*, 2000, p. 1417.
[13] ZOLLINGER, J.—LAPIN, J.—DALOZ, D.—COMBEAU, H.: Intermetallics, *15*, 2007, p. 1343.
[14] LAPIN, J.: Intermetallics, *14*, 2006, p. 115.
[15] LAPIN, J.—NAZMY, M.: Mater. Sci. Eng. A, *380*, 2004, p. 298.
[16] GURRAPPA, I.: Mater. Charact., *51*, 2003, p. 131.
[17] ALBRECHT, J.: Mater. Sci. Eng. A, *263*, 1999, p. 176.
[18] KARLÍK, M.—KRATOCHVÍL, P.—JANEČEK, M.—SIEGL, J.—VODIČKOVÁ, V.: Mater. Sci. Eng. A, *289*, 2000, p. 182.
[19] KRATOCHVÍL, P.—PEŠIČKA, J.—HAKL, J.—VLASÁK, T.—HANUS, P.: J. Alloys Compd., *378*, 2004, p. 258.
[20] KARLÍK, M.—NEDBAL, I.—SIEGL, J.—PRAHL, J.: J. Alloys Compd., *378*, 2004, p. 263.
[21] KUPKA, M.: Intermetallics, *14*, 2006, p. 149.
[22] GEBURA, M.—LAPIN, J.: In: 17$^{\text{th}}$ International Conference on Metallurgy and Materials Metal 2008. Ed.: Tanger, s.r.o., Ostrava 2008, CD ROM.
[23] HAKL, J.—VLASÁK, T.—LAPIN, J.: Kovove Mater., *45*, 2007, p. 177.
[24] NABARRO, F. R. N.: Metall. Mater. Trans. A, *27*, 1996, p. 513.
[25] LAPIN, J.—ONDRÚŠ, Ľ.—NAZMY, M.: Intermetallics, *10*, 2002, p. 1019.
[26] BALDAN, A.: J. Mater. Sci., *37*, 2002, p. 2379.
[27] KARUNARATNE, M. S. A.—CARTER, P.—REED, R. C.: Acta Mater., *49*, 2001, p. 861.
[28] POLLOCK, T. M.—ARGON, A. S.: Acta Metall. Mater., *40*, 1992, p. 1.
[29] MA, S.—SEETHARAMAN, V.—MAJUMDAR, B. S.: Acta Mater., *56*, 2008, p. 4102.
[30] BENYOUCEF, M.—COUJOU, A.—PETTINARI-STURMEL, F.—RAUJOL, S.—BOUBKER, B.—CLEMENT, N.: Sādhanā, *28*, 2003, p. 129.
[31] LAPIN, J.—DELANNAY, F.: Metal. Mater. Trans. A, *26A*, 1995, p. 2053.
[32] SIEBÖRGER, D.—KNAKE, H.—GLATZEL, U.: Mater. Sci. Eng. A, *298*, 2001, p. 26.
[33] LUKÁŠ, P.—ČADEK, J.—KUNZ, L.—SVOBODA, M.—KLUSÁK, J.: Kovove Mater., *43*, 2005, p. 5.
[34] GLATZEL, U.: Scripta Metall. Mater., *31*, 1994, p. 291.
[35] LAPIN, J.—DUBIEL, B.—NAZMY, M.—GEBURA, M.: (in preparation).
[36] CAHN, R. W.—HAASEN, P.—KRAMER, E. J.: Materials Science and Technology. Volume 6 – Plastic Deformation and Fracture of Materials. Vol. Ed.: Mughrabi, H. D-6940 Weinheim, VCH Verlagsgesellschaft mbH 1993, p. 311.
[37] ARDELL, A. J.: Metall. Trans. A, *16A*, 1985, p. 2131.